Identification of U^P47 in three thermophilic archaea, one mesophilic archaeon, and one hyperthermophilic bacterium

PHILIPPE WOLFF,[1] ANTONY LECHNER,[1] LOUIS DROOGMANS,[2] HENRI GROSJEAN,[2] and ERIC WESTHOF[1]

[1]Architecture et Réactivité de l'ARN, Institut de Biologie Moléculaire et Cellulaire du CNRS, Université de Strasbourg, F-67084 Strasbourg, France
[2]Laboratoire de Chimie Biologique, Université Libre de Bruxelles, Institut Labiris, Anderlecht B-1070, Belgium

ABSTRACT

Analysis of the profile of the tRNA modifications in several *Archaea* allowed us to observe a novel modified uridine in the V-loop of several tRNAs from two species: *Pyrococcus furiosus* and *Sulfolobus acidocaldarius*. Recently, Ohira and colleagues characterized 2′-phosphouridine (U^P) at position 47 in tRNAs of thermophilic *Sulfurisphaera tokodaii*, as well as in several other archaea and thermophilic bacteria. From the presence of the gene *arkI* corresponding to the RNA kinase responsible for U^P47 formation, they also concluded that U^P47 should be present in tRNAs of other thermophilic *Archaea*. Reanalysis of our earlier data confirms that the unidentified residue in tRNAs of both *P. furiosus* and *S. acidocaldarius* is indeed 2′-phosphouridine followed by m^5C48. Moreover, we find this modification in several tRNAs of other *Archaea* and of the hyperthermophilic bacterium *Aquifex aeolicus*.

Keywords: mass spectrometry; *Archaea*; tRNA; modifications; hyperthermophiles; *A. aeolicus*

INTRODUCTION

In a previous work, we have established the profile of the tRNA modifications of several *Archaea* (Wolff et al. 2020). We used mass spectrometry to localize and characterize the tRNA modifications. We discovered some modifications that we did not manage to fully identify chemically. One of them was attributed to position U47 in some tRNAs from *Pyrococcus furiosus* (a hyperthermophilic archaeon belonging to the phylum Thermococcales) and from the thermoacidophile *Sulfolobus acidocaldarius* (belonging to the phylum Sulfolobales) with an assumed nucleoside mass of 338 kDa (noted as xU47). The recent identification by mass spectrometry of 2′-phosphouridine (U^P47, nucleoside mass of 324 kDa) at position 47 of tRNAs of thermoacidophilic crenarcheon *Sulfurisphaera tokodaii*, and by extension in tRNAs from several other thermophilic *Archaea* (Ohira et al. 2022), prompted us to reanalyze our data.

We now find that the putative modified uridine (xU47) in *P. furiosus* and *S. acidocaldarius* corresponds indeed to a 2′-phosphouridine (U^P) that is followed by 5-methylated C48 (accounting for the 14 kDa difference between the observed nucleoside masses, 338 and 324, respectively) as in *S. tokodaii* (Ohira et al. 2022). Moreover, we also find that U^P is present at position 47 of the mesophilic archaeon *Methanococcus maripaludis*, in the hyperthermophilic and acidophilic archaeon *Saccharolobus shibatae* and interestingly also in the hyperthermophilic bacterium *Aquifex aeolicus*.

RESULTS AND DISCUSSION

MSMS data

The interpretation of the first MSMS data of the oligonucleotides obtained by RNase T_1 of tRNAs from several archaea (the fragment of interest always started with 5′-U47C48) allowed us to conclude on the presence of xU47C48. Indeed, the expected ions corresponding to the fragmentation between U47 and C48 (fragments c_1 and y_5 in the example [see Fig. 1]) were missing in the spectra. Instead, we only found a fragment of 704.1 kDa corresponding to the dinucleotide xU47C48. On the other hand, RNase A analysis of the same tRNAs revealed the presence of the fragment ion carrying the same unknown modification, with a dinucleotide fragment of 722.1 kDa

Corresponding authors: e.westhof@ibmc-cnrs.unistra.fr, p.wolff@ibmc-cnrs.unistra.fr

Article is online at http://www.rnajournal.org/cgi/doi/10.1261/rna.079546.122. Freely available online through the *RNA* Open Access option.

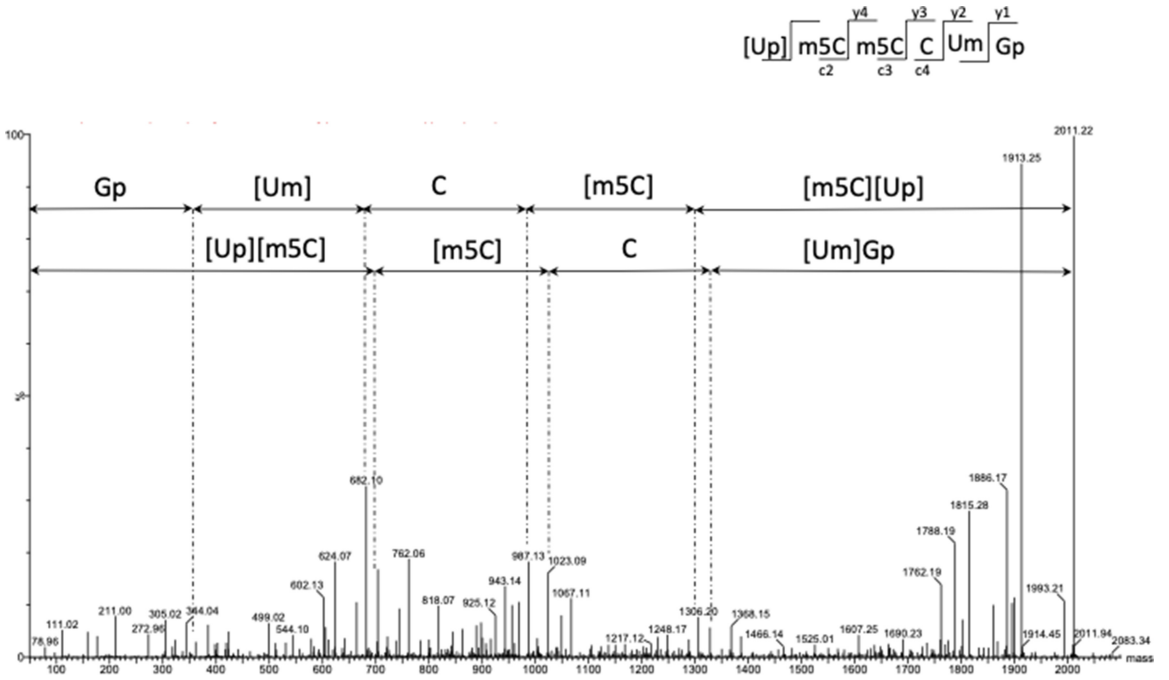

FIGURE 1. Deconvoluted MS/MS sequencing spectrum (Wolff et al. 2020) (U^P)(m^5C)(m^5C)C(Um)Gp of Ini-tRNA-CAU from *S. acidocaldarius* after T_1 digestion ($m/z = 1005.2$, $z = -2$). No ion fragment of U^P is detected, probably due to the protection conferred by 2′-phosphate and insufficient CID energy, but ions c_2 (704) and y_4 (1306) corresponding to the dinucleotide (Wolff et al. 2020) were detected. See Table 2 for localization of the fragment.

(corresponding to xU47C48-3′p). This allows us to conclude that the modification carried by the U47 prevents RNase A cleavage. Moreover, because C48 was cleaved by the RNase A, it suggests also that C48 was likely unmodified. This leads us to conclude that the fragment generated by RNase A corresponds to xU47C48.

After publication of the first known internal post-transcriptional phosphorylation of uridine at position 47 (Ohira et al. 2022), we performed complementary experiments to determine whether this phosphoryl adduct is also present in our tRNAs studied previously (Wolff et al. 2020). To confirm the presence of U^P47, the RNase T_1 fragment oligonucleotides obtained from purified initiator $tRNA^{Met}$ from *S. acidocaldarius* was treated with bacterial alkaline phosphatase (BAP) followed by MS analysis. BAP can hydrolyze 5′- and 3′-phosphate but also 2′-phosphate (Ohira et al. 2022). As a matter of fact, based on the CID sequencing spectrum, the RNA fragment (U^P)(m^5C)(m^5C)C(Um)Gp (Fig. 1), detected without BAP treatment, was converted to U(m^5C)(m^5C)C(Um)G (Fig. 2).

The data provided by these additional experiments allow us to conclude that the previously found xU47 was in fact U^P followed by m^5C. The mass of U^P (324 kDa) added to the mass of the methyl group of m^5C (14 Da) corresponds to the mass of the reported xU (338 kDa, see above). The missing CID fragmentation ions resulting from cleavage between U47 and C48, mentioned above (Fig. 3), could be explained by the presence of 2′-O-phosphate in U47 (Fig. 3A). We hypothesize that the presence of a 2′-phosphate group may protect the phosphodiester link against CID fragmentation, as it is the case with 2′-O-methyl (Smith and Brodbelt 2011). Hence, the fragmentation is less favorable resulting in weaker or suppressed MSMS peaks (Fig. 3B). In the case of Ohira et al. (2022), the presence of U^P47 was also detected in *S. acidocaldarius* after digestion by nuclease P_1 and LC/MS analysis (see also Table 2 in this paper).

Presence of U^P47 in various tRNAs

In *Sulfurisphaera tokodaii*, U^P47 was observed in Lys-tRNA-UUU, Thr-tRNA-UGU, Gly-tRNA-UCC, Arg-tRNA-UCG, Pro-tRNA-GGG, Ile2-tRNA-CAU, and Phe-tRNA-GAA and was not observed in Gln-tRNA-UGG, Cys-tRNA-GCA, Leu-tRNA-UAG, nor Ser-tRNA-GGA (Ohira et al. 2022). Here, we find U^P47 in Initiator Met-tRNA-CAU of all four archaea that we analyzed, as well as in Met-tRNA-CAU of *M. maripaludis* and *P. furiosus* (Tables 1, 2). We further find U^P47 in Arg-tRNA-UCG, Asn-tRNA-GUC, Thr-tRNA-GGU, Val-tRNA-GAC, Gly-tRNA-GCC (see Supplemental Figs. S1–S4 for selected annotated spectra). As noticed (Ohira et al. 2022), all tRNAs with U^P47 have 5 nt in the V-loop and U^P47 is always followed by C48. Except in the archaeon *M. maripaludis* and bacterium *A. aeolicus* where it is unmodified, C48 is methylated at position 5 (m^5C48). Further, in *A. aeolicus*, position 46 is m^7G46. In five tRNAs, position 49 is

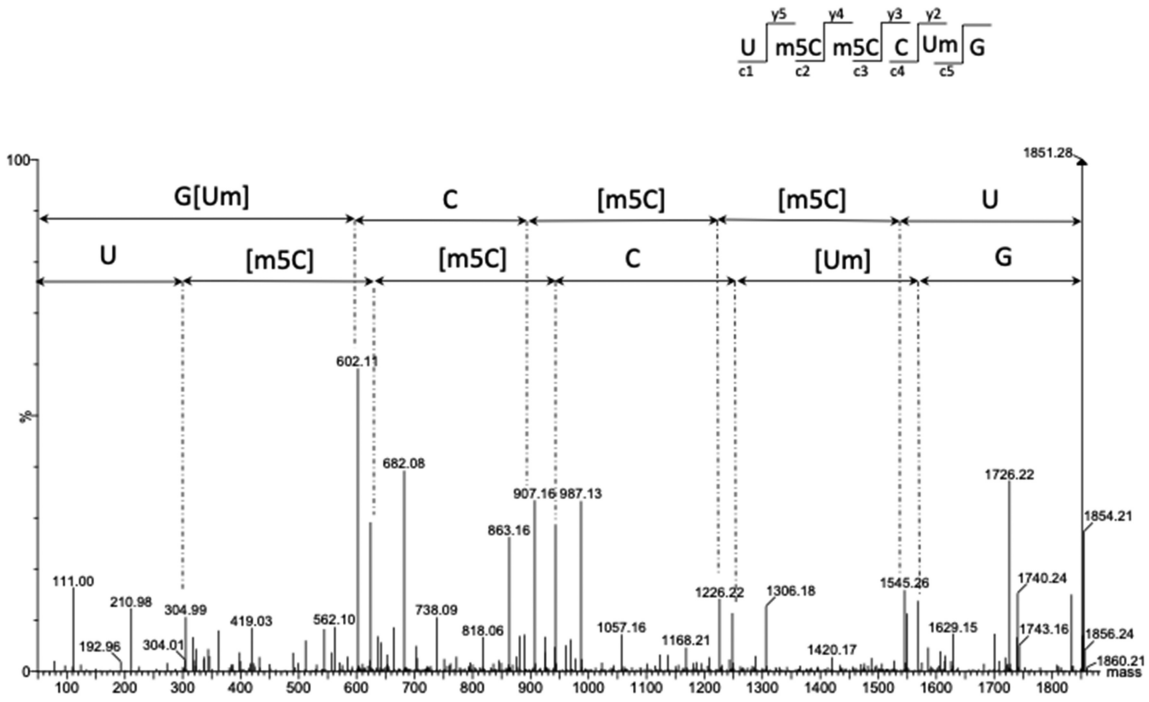

FIGURE 2. Deconvoluted MS/MS sequencing spectrum U(m^5C)(m^5C)C(Um)G of Ini-tRNA-CAU from *S. acidocaldarius* after T_1 and BAP digestion (*m/z* = 925.13, z = −2). The spectrum clearly shows the ion fragments corresponding to U47 without phosphate (c_1 = 305 and y_5 = 1545). See Table 2 for localization of the fragment.

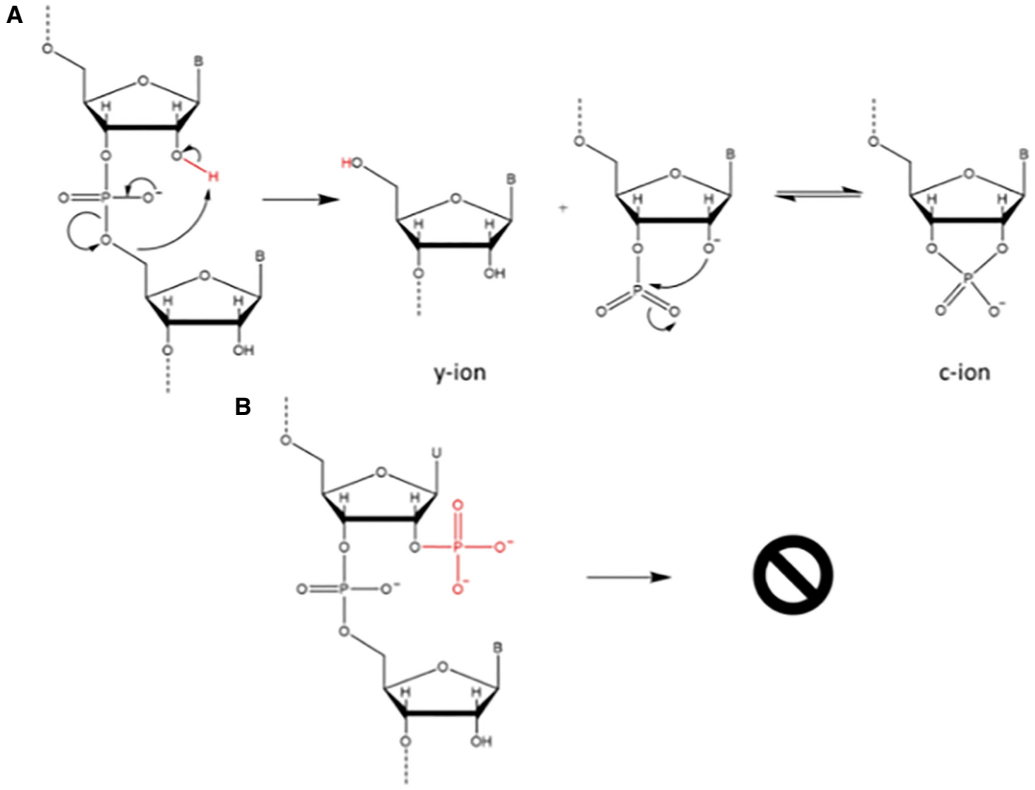

FIGURE 3. (*A*) Mechanism of formation of c-ions and y-ions by CID showing the involvement of 2′-OH during fragmentation (see also Tromp and Schurch 2005). (*B*) Scheme showing that CID formation of c-ions and y-ions is less favorable due to O2′-phosphate of $U^{p}47$.

TABLE 1. List of tRNAs containing U^P47 identified by LC-MSMS with relevant LC/MS data and sequences

Species	tRNA	U47	C48	Precursor ion *m/z*	Calculated mass (Da)	Sequence	RNase	Production U47C48	Production *m/z* (charge)	Arki homolog
Methanococcus maripaludis	Arg UCU	U^P	C	1208.14 (−2)	2418.3	GGGGA[U^P]Cp	A	y_2	708.1 (−1)	Serine/theronine protein kinase
	Asn GUU	U^P	C	863.09 (−2)	1728.2	AGG[U^P]Cp	A	y_2	708.1 (−1)	WP_013999910.1
	Lni CAU	U^P	C	1200.13 (−2)	2402.3	GGAGA[U^P]Cp	A	y_2	708.1 (−1)	
	Met CAU	U^P	C	1372.67 (−2)	2747.3	GAGAGG[U^P]Cp	A	y_2	708.1 (−1)	
Pyrococcus furiosus	Lni CAU	U^P	m^5C	1215.15 (−2)	2432.3	GGAGG[U^P][m^5C]p	A	y_2	722.1 (−1)	Serine/theronine protein kinase
	Met CAU	U^P	m^5C	1379.67 (−2)	2761.3	GGGAGA[U^P][m^5C]p	A	y_2	722.1 (−1)	WP_014835421.1
	Thr GGU	U^P	m^5C	870.09 (−2)	1742.2	AGG[U^P][m^5C]p	A	y_2	722.1 (−1)	
Sulfolobus acidocaldarious	Lni CAU	U^P	m^5C	1005.1 (−2)	2012.2	[U^P][m^5C][m^5C]C[Um]Gp	T_1	c_2	704.1 (−1)	Serine/theronine protein kinase
	Gly GCC	U^P	m^5C	1379.67 (−2)	2761.3	AGGAGG[U^P][m^5C]p	A	y_2	722.1 (−1)	WP_015385591.1
	Val GAC	U^P	m^5C	1191.14 (−2)	2384.3	AGAAA[U^P][m^5C]p	A	y_2	722.1 (−1)	
Saccharolobus shibatae	Pro UGG	U^P	m^5C	697.56 (−2)	1397.1	A[U^P][m^5C]Gp	T_1	/	/	Serine/theronine protein kinase
	lni CAU	U^P	m^5C	1019.11 (−2)	2040.2	[U^P][m^5C][m^5C][ac^4C]UGp	T_1	c_2	704.1 (−1)	WP_218266278.1
Aquifex aeolicus	Pro GGG	U^P	C	1207.15 (−2)	2416.3	AGAG[m^7G][U^P]Cp	A	y_2	708.1 (−1)	Hypothetical protein
	Val GAC	U^P	C	1215.13 (−2)	2267.2	GGAG[m^7G][U^P]Cp	A	y_2	708.1 (−1)	WP_010880344.1

The accession numbers of the potential *arkI* homologs in the various archaeal species are indicated in the last column (based on BlastP searches). The presence of *arkI* homologs was previously shown in Ohira et al. (2022).

TABLE 2. Compilation of modified tRNA sequences from *M. maripaludis*, *P. furiosus*, *S. acidocaldarius*, *S. shibatae*, and *A. aeolicus*

	Acc-stem		D-stem	D-loop	D-stem		Ac-stem	Ac-loop	Ac-stem	V-region	T-stem	T-loop	T-stem	Acc-stem		CCA
	1	8	10	14	22	26	27	32	39	44	49	54	61	66	73	74
M. maripaludis																
Arg UCU	GGGCCCG	UG	GCCU	AGUCUGGAUA	CGGC	A	CCGGC	CUUCU[t6A]A	GCCGG	GG——A[Up]C	GGGGG	[m1Y]UCG[m1A]AU	CCCUC	CGGGUCC	G	CC-
Asn GUU	GCCUCCU	UA	GCUC	A[G+]UAGGUAG	CAGC	[m2,2G]	ACGGA	CUGUU[hn6A]A	UCCGU	AG——G[Up]C	GCAGG	UUCGAGC	CCUGC	AGGAGGC	G	CCA
Ini CAU	AGCGAGG	UA	GGGU	A[G+]CCAGGCCUA	UCCC	G	CCGGG	CUCAUAA	CCCGG	AG——A[Up]C	AGAAG	UUCAAAU	CUUCU	CCUCGCU	A	CCA
Met CAU	GCCGAGG	UG	GCUU	A[G+]GCUGGUUA	UAGC	[m2,2G]	CUCGG	CU[Cm]AU[hn6A]A	CCGAG	AG——G[Up]C	GGGGG	[m1Y]U[Cm][m1I]AGU	CCCCC	CCUCGGC	-	
P. furiosus																
Ini CAU	AGCGG[m2G]G	U[Gm]	[Gm]GGC/[Cm]	A[G+]CUAGGAG[Um]	[Gm]CCC	[m2,2G]	CCGGG	CUCAUAA	CCCGG	AG——G[Up][m5C]	CGAGG	[m5s2U]U[Cm][m1I][m1A]AU	CCUCG	GCCCGCU	A	CCA
Met CAU	GCCGG[m2,2G]G	UA	GCUU	AGCCUGGUCA	AAGC	[m2,2Gm]	[m5C]CCGG	CU[Cm]AU[m6t6A]A	CCGGG	AG——A[Up][m5C]	CGGGG	[m5s2U]U[Cm]G[m1A]AG	CCC[ac4C]G	CCCCGGC	A	CCA
Thr GGU	GCCCCGG	UG	GCUC	A[G+]CC/[s2C]UGGUA	[Gm]AGC	[m2,2Gm]	GCCGC	UUGGU[t6A]/[m6t6A]A	GCGGC	AG——G[Up][m5C]	[m5C]CGGG	[m5U]/[m5s2U]U[Cm][m1I][m1A]AG	CCGGG	CCG/[Gm]GGGC	U	CCA
S. acidocaldarius																
Val GAC	GGGCCCG	UC	[m2G]UCU	A[G+]C[Cm]UGGUU-A	GGA[Cm]	[m2,2G]	CUGCC	[Cm]UGAC[m1G]C	GGCAG	AA——A[Up][m5C]	[m5C][Um]GGG	[s2U]U[Cm][m1I][m1A]GU	CCCAG	CGGGCCC	A	
Gly GCC	GCGGCCG	UA	GUCU	A[G+]CCUGG[Am]UUA	GGAC	[m2,2G]	CCUGC	CUGCCAC	GCAGG	AG——G[Up][m5C]	C[Cm]GGG	[s2U]U[Cm][m1I][m1A]AU	CCCGG	CGGUCGC	A	
Ini CAU	AGCGGCG	U[m1A]	[m2G]GGA	A[G+]CCUGGUA	UCCC	[m2,2Gm]	CA[Gm]GG	[Cm]UCAUAA	CCCUG	AG——G[Up][m5C]	[m5C]C[Um]GG	[s2U]U[Cm][m1I][m1A]AU	C[Cm]AGG	CGCCGCU	A	
S.shibatae																
Ini CAU	AGCGGGG	UG	GGCU	A[G+]C[Cm]UGGUAA	GGCC	G	CGGGG	[Cm]UCAUAA	CCCCG	AG——G[Up][m5C]	[m5C][ac4C]UGG	UU[Cm][Im][m1A]AU	CCAGG	CCCCGCU	A	CCA
Pro GGG	GGGGCCG	UA	GUCU	A[G+]CUUGG[Am]CUA	GGAU	G	CCAGC	CUGGGGC	GCUGG	UG——G[Up][m5C]	[m5C][Cm]GGG	UU[Cm][Im][m1A]AU	CCCGG	CGGCCCC	A	
A. aeolicus																
Pro GGG	CGGGGUG	UA	GCGC	AGGU-GGU--A	GCGC	[m2,2G]	[m5C]UGGC	[Am]UGGG[m1G]G	GCCAG	AG——[m7G][Up]C	GCCGG	UUCGAGU	CCGGU	CACCCCG	A	CCA
Val GAC	AGGCGCG	UA	GCUC	AGUA[Gm]GG--A	GAGC	[m2,2G]	[m5C]CGGC	[Cm]CGAC[m6A]C	GCCGG	AG——[m7G][Up]C	GGGGG	[m5s2U]UCA[m1A]GU	CCCCC	CGCGCCU	A	CCA
S.tokodaii																
Arg UCG	GGACCCG	UA	GCUC	AGCCAGGAU-A	GAGC	G	CCGGC	CUUCGGA	GCCGG	UG——G[Up][m5C]	[m5C][Cm]GGG	UUCAAAU	CCCGG	CGGGUCC	G	--
Gly UCC	GCGGCCG	UC	GUCU	AGUCUGGAUUA	GGAC	G	CUGGC	CUUCCAA	GCCAG	UA——A[Up][m5C]	[m5C][Cm]GGG	UUCAAAU	CCCGG	CGGCCGC	A	--
Lys UUU	GGGCCCG	UA	GCUC	AGCCAGGU--A	GAGC	G	GCGGG	CUUUUAA	CCCGU	AG——G[Up][m5C]	[m5C][Cm]GGG	UUCAAAU	CCCGG	CGGGCCC	G	--
Phe GAA	GCCGCCG	UA	GCUC	AGCCCGGG--A	GAGC	G	CCCGG	CUGAAGA	CCGGG	UU——G[Up][m5C]	[m5C]CGGG	UUCAAGU	CCCCG	CGGCGGC	A	--
Pro GGG	GGGACCG	UC	GUCU	AGCCUGGACUA	GGAU	G	CAGGC	CUGGGGC	GCCUG	UG——G[Up][m5C]	[m5C][Cm]GGG	UUCAAAU	CCCGG	CGGUCCC	A	--
Thr UGU	GCCGCUG	UA	GCUC	AGCCUGGUU-A	GAGC	G	CCGGC	CUUGUAA	GCCGG	CG——G[Up][m5C]	[m5C]GGGG	UUCAAAU	CCCCG	CAGCGGC	U	--
Ile CAU	GGGCCCG	UA	GCUU	GGUAGA	GCGC	C	CCGG	CUCAUAA	CCGGG	UG——G[Up][m5C]	[m5C]GGGG	UUCAAGU	CCCCG	CGGGCCC	A	
Val GAC	GGGCC[ac4C]G	[s4U]C	[m2G]UC[Y]	A[G+]C[Cm]UGGUU-A	GGAC	[m2,2G]	CCGCC	[Cm]UGAC[m1G]C	GGCGG	AG——G[Up][m5C]	[m5C][Um]GGG	[s2U][Y][Cm][m1I][m1A]GU	CCCAG	CGGGCCC	A	--

For comparisons, the data for *S. tokodaii* are also shown; they are from Ohira et al. (2022). Nucleotides in red indicate fragments obtained by RNase T1, and/or RNase A, and/or RNase U2 digestion, while those in black represent regions that could not be analyzed. The modified nucleotides detected and analyzed are shown in green.

also methylated at position 5, resulting in m^5C49. Furthermore, in *S. shibatae* Initiator Met-tRNA-CAU, ac^4C is detected at position 50. Expected modifications typical of *Archaea* are also detected (Table 2; see also Pang et al. 1982; Gupta 1984; Edmonds et al. 1991; Watanabe et al. 1997; Urbonavicius et al. 2006; Grosjean et al. 2008; Tomikawa et al. 2013; Hirata et al. 2019; Yu et al. 2019; Rose et al. 2020; Sas-Chen et al. 2020; Wolff et al. 2020; Ohira et al. 2022).

Conclusions

To date the presence of post-transcriptional internal phosphorylation of a nucleotide in tRNA as U^P47 was reported in hyperthermophilic *Archaea* and in *Nitrososphaera viennensis*, a mesophilic archaeon (Ohira et al. 2022). Here, we show that this modification is also present in the mesophilic archaeon *M. maripaludis*. Most interestingly we find this modification in *A. aeolicus*, a hyperthermophilic bacterium. The presence of U^P47 in several thermophilic archaea and *A. aeolicus* was only suspected from the presence in the genomes of gene *arkI* homologs coding for specific U47 kinase. The recombinant form of this newly identified modification enzyme from *T. kodakarensis* can catalyze base phosphorylation of U47 in vitro in the presence of ATP (Ohira et al. 2022). In Table 1, potential *arkI* homologs, annotated as Ser/Thr kinases, in the various archaeal species studied are indicated (see also Ohira et al. 2022). In *A. aeolicus*, the gene (aq_578) is in a region of the chromosome containing tRNA genes with, as direct neighbor, the polypeptide deformylase gene. In sum, these results show that this internal nucleotide phosphorylation is a modification not only present in thermophilic but also in mesophilic archaea (as in the mesophilic bacterium *Nautilia profundicola* where *ArkI* has U^P-modifying activity in vitro, Ohira et al. 2022) and in hyperthermophilic *Bacteria*. The present note completes our previous report on tRNA modifications in *Archaea* (Wolff et al. 2020).

MATERIALS AND METHODS

tRNA isolation by 2D-gel electrophoresis

tRNA isoacceptors were isolated using two-dimensional gel electrophoresis as previously described (Wolff et al. 2020). Briefly, the total tRNA of each organism was briefly heated at 90°C. Then, samples were separated in a first-dimension gel under denaturing conditions using 12.5% polyacrylamide gel, 1× TBE and 8 M urea, followed by a second dimension under semidenaturing conditions using 20% polyacrylamide gel, TBE 1× and 4 M urea at room temperature. Gels were stained with an ethidium bromide solution (10 $\mu g/L^{-1}$) for about 10 min. Finally, spots containing tRNAs were visualized and excised under UV light (302 nm).

In-gel RNase digestion of tRNAs

Gel spots containing tRNAs were first desalted by several washes (at least eight) with 100 µL 200 mM NH_4AcO and gel spots were dried under vacuum. For RNase T_1 and RNase A hydrolyzes, gel pieces were rehydrated by 20 µL of 0.1 $U/\mu L^{-1}$ of RNase T_1 or by 20 µL of 0.01 $U/\mu L^{-1}$ of RNase A (Thermo Fisher Scientific) in 100 mM NH_4AcO (pH is not adjusted). For RNase U_2 digestion, spots were digested by using 50 µL of RNase U_2 (homemade) at 0.3 $ng/\mu L^{-1}$ in 50 mM NH_4AcO (pH 5.3) and incubated for 45 min at 65°C. After digestion, supernatants were dried under vacuum. Bacterial alkaline phosphatase (BAP) dephosphorylation was performed by adding 10U of BAP to the RNase mixture and incubating for 3 h at 37°C.

NanoLC-MS/MS of RNA oligonucleotides

Pellets containing RNase digestion products were resuspended in 3 µL of milli-Q water and separated on an Acquity peptide BEH C18 column (130 Å, 1.7 µm, 75 µm × 200 mm) using a nanoAcquity system (Waters). The analyses were performed with an injection volume of 3 µL. The column was equilibrated in buffer A containing 7.5 mM TEAA (Triethylammonium acetate), 7.0 mM TEA (Triethylammonium), and 200 mM HFIP (Hexafluoroisopropanol) at a flow rate of 300 nL/min^{-1}. Oligonucleotides were eluted using a gradient from 15% to 35% of buffer B (100% methanol) for 2 min followed by an increase of buffer B to 50% in 20 min. MS and MS/MS analyses were performed using SYNAPT G2-S (hybrid quadrupole time-of-flight mass spectrometer) from Waters Corporation. All experiments were performed in negative mode with a capillary voltage set at 2.6 kV and a sample cone voltage set at 30 V. Source was heated to 130°C. The samples were analyzed over an *m/z* range from 550 to 1600 for the full scan, followed by fast data direct acquisition scan (Fast DDA). Collision-induced dissociation (CID) experiments were achieved using Ar.

Data analysis

All MSMS spectra were deconvoluted using MassLynx software from Waters and manually sequenced by following the y and/or c series (w ions were also useful when sequencing was difficult or to confirm a sequence). tRNA identification was done by comparisons with the genomic sequences obtained from GtRNAdb (http://gtrnadb.ucsc.edu/) (Chan and Lowe 2016). Data about nucleoside modification were obtained from Modomics database (https://iimcb.genesilico.pl/modomics/modifications) (Boccaletto et al. 2022).

SUPPLEMENTAL MATERIAL

Supplemental material is available for this article.

ACKNOWLEDGMENTS

The project was supported by the French National Program Investissement d'Avenir (Labex NetRNA) administered by the Agence Nationale de la Recherche (ANR-10-LABX-0036_NETRNA). This work of the Interdisciplinary Thematic Institute IMCBio, as part of the ITI 2021-2028 program of the University of Strasbourg, CNRS and Inserm, was supported by IdEx Unistra (ANR-10-IDEX-0002), and by SFRI-STRAT'US project (ANR 20-SFRI-0012) and EUR IMCBio (ANR-17-EURE-0023) under the framework of the French Investments for the Future Program. Anthony Lechner was supported by Fonds Régional de Coopération pour la Recherche (Region Grand Est, EpiRNA).

Received December 6, 2022; accepted January 19, 2023.

REFERENCES

Boccaletto P, Stefaniak F, Ray A, Cappannini A, Mukherjee S, Purta E, Kurkowska M, Shirvanizadeh N, Destefanis E, Groza P, et al. 2022. MODOMICS: a database of RNA modification pathways. 2021 update. *Nucleic Acids Res* **50:** D231–D235. doi:10.1093/nar/gkab1083

Chan PP, Lowe TM. 2016. GtRNAdb 2.0: an expanded database of transfer RNA genes identified in complete and draft genomes. *Nucleic Acids Res* **44:** D184–D189. doi:10.1093/nar/gkv1309

Edmonds CG, Crain PF, Gupta R, Hashizume T, Hocart CH, Kowalak JA, Pomerantz SC, Stetter KO, McCloskey JA. 1991. Posttranscriptional modification of tRNA in thermophilic archaea (Archaebacteria). *J Bacteriol* **173:** 3138–3148. doi:10.1128/jb.173.10.3138-3148.1991

Grosjean H, Gaspin C, Marck C, Decatur WA, de Crecy-Lagard V. 2008. RNomics and modomics in the halophilic archaea *Haloferax volcanii*: identification of RNA modification genes. *BMC Genomics* **9:** 470. doi:10.1186/1471-2164-9-470

Gupta R. 1984. *Halobacterium volcanii* tRNAs. Identification of 41 tRNAs covering all amino acids, and the sequences of 33 class I tRNAs. *J Biol Chem* **259:** 9461–9471. doi:10.1016/S0021-9258(17)42723-2

Hirata A, Suzuki T, Nagano T, Fujii D, Okamoto M, Sora M, Lowe TM, Kanai T, Atomi H, Suzuki T, et al. 2019. Distinct modified nucleosides in tRNA^{Trp} from the hyperthermophilic archaeon *Thermococcus kodakarensis* and requirement of tRNA $m^2G10/m^2{}_2G10$ methyltransferase (Archaeal Trm11) for survival at high temperatures. *J Bacteriol* **201:** e00448-19. doi:10.1128/JB.00448-19

Ohira T, Minowa K, Sugiyama K, Yamashita S, Sakaguchi Y, Miyauchi K, Noguchi R, Kaneko A, Orita I, Fukui T, et al. 2022. Reversible RNA phosphorylation stabilizes tRNA for cellular thermotolerance. *Nature* **605:** 372–379. doi:10.1038/s41586-022-04677-2

Pang H, Ihara M, Kuchino Y, Nishimura S, Gupta R, Woese CR, McCloskey JA. 1982. Structure of a modified nucleoside in archaebacterial tRNA which replaces ribosylthymine. 1-Methylpseudouridine. *J Biol Chem* **257:** 3589–3592. doi:10.1016/S0021-9258(18)34820-8

Rose S, Auxilien S, Havelund JF, Kirpekar F, Huber H, Grosjean H, Douthwaite S. 2020. The hyperthermophilic partners *Nanoarchaeum* and *Ignicoccus* stabilize their tRNA T-loops via different but structurally equivalent modifications. *Nucleic Acids Res* **48:** 6906–6918. doi:10.1093/nar/gkaa411

Sas-Chen A, Thomas JM, Matzov D, Taoka M, Nance KD, Nir R, Bryson KM, Shachar R, Liman GLS, Burkhart BW, et al. 2020. Dynamic RNA acetylation revealed by quantitative cross-evolutionary mapping. *Nature* **583:** 638–643. doi:10.1038/s41586-020-2418-2

Smith SI, Brodbelt JS. 2011. Hybrid activation methods for elucidating nucleic acid modifications. *Anal Chem* **83:** 303–310. doi:10.1021/ac102411a

Tomikawa C, Ohira T, Inoue Y, Kawamura T, Yamagishi A, Suzuki T, Hori H. 2013. Distinct tRNA modifications in the thermo-acidophilic archaeon, *Thermoplasma acidophilum*. *FEBS Lett* **587:** 3575–3580. doi:10.1016/j.febslet.2013.09.021

Tromp JM, Schurch S. 2005. Gas-phase dissociation of oligoribonucleotides and their analogs studied by electrospray ionization tandem mass spectrometry. *J Am Soc Mass Spectrom* **16:** 1262–1268. doi:10.1016/j.jasms.2005.03.024

Urbonavicius J, Armengaud J, Grosjean H. 2006. Identity elements required for enzymatic formation of N^2,N^2-dimethylguanosine from N^2-monomethylated derivative and its possible role in avoiding alternative conformations in archaeal tRNA. *J Mol Biol* **357:** 387–399. doi:10.1016/j.jmb.2005.12.087

Watanabe M, Matsuo M, Tanaka S, Akimoto H, Asahi S, Nishimura S, Katze JR, Hashizume T, Crain PF, McCloskey JA, et al. 1997. Biosynthesis of archaeosine, a novel derivative of 7-deazaguanosine specific to archaeal tRNA, proceeds via a pathway involving base replacement on the tRNA polynucleotide chain. *J Biol Chem* **272:** 20146–20151. doi:10.1074/jbc.272.32.20146

Wolff P, Villette C, Zumsteg J, Heintz D, Antoine L, Chane-Woon-Ming B, Droogmans L, Grosjean H, Westhof E. 2020. Comparative patterns of modified nucleotides in individual tRNA species from a mesophilic and two thermophilic archaea. *RNA* **26:** 1957–1975. doi:10.1261/rna.077537.120

Yu N, Jora M, Solivio B, Thakur P, Acevedo-Rocha CG, Randau L, de Crecy-Lagard V, Addepalli B, Limbach PA. 2019. tRNA modification profiles and codon-decoding strategies in *Methanocaldococcus jannaschii*. *J Bacteriol* **201:** e00690-18. doi:10.1128/JB.00690-18